Statistical Analysis and Optimization of Factors Affecting the Spring-back Phenomenon in UVaSPIF Process Using Response Surface Methodology

M. Vahdati* & R. A. Mahdavinejad
Department of Mechanical Engineering,
University of Tehran, Iran
E-mail: vahdati@ut.ac.ir, mahdavin@ut.ac.ir
*Corresponding author

S. Amini
Department of Mechanical Engineering,
University of Kashan, Iran
E-mail: amini.s@kashanu.ac.ir

Abstract: Ultrasonic Vibration assisted Single Point Incremental Forming (UVaSPIF) process is an attractive and adaptive method in which a sheet metal is gradually and locally formed by a vibrating hemispherical-head tool. The ultrasonic excitation of forming tool reduces the average of vertical component of forming force and spring-back rate of the formed sample. The spring-back phenomenon is one of the most important geometrical errors in SPIF process, which appear in the formed sample after the process execution. In the present article, a statistical analysis and optimization of effective factors on this phenomenon is performed in the UVaSPIF process based on DOE (Design of Experiments) principles. For this purpose, RSM (Response Surface Methodology) is selected as the experiment design technique. The controllable factors such as vertical step size, sheet thickness, tool diameter, wall inclination angle, and feed rate is specified as input variables of the process. The obtained results from ANOVA (Analysis of Variance) and regression analysis of experimental data, confirm the accuracy of mathematical model. Furthermore, it is shown that the linear, quadratic, and interactional terms of the variables are effective on the spring-back phenomenon. To optimize the spring-back phenomenon, the finest conditions of the experiment are determined using desirability method, and statistical optimization is subsequently verified by conducting the confirmation test.

Keywords: RSM, Single Point Incremental Forming, Spring-back, Ultrasonic Vibration

Biographical notes: M. Vahdati is PhD candidate of mechanical engineering. His current research focuses on incremental sheet metal forming processes. **R. A. Mahdavinejad** is associated professor of mechanical engineering. His research interest is in traditional and non-traditional processes. **S. Amini** is assistant professor of mechanical engineering. His research interest includes ultrasonic and machining processes.

1   INTRODUCTION

Nowadays, production industries need to use economical and flexible processes to enable them to meet the market demands in a competitive environment with a minimum cost and time. Thus, researchers have considered the investigation of operational methods in order to produce the primary sample and develop new products. Single Point Incremental Forming (SPIF) process has been introduced as an attractive and adaptive method among the rapid prototyping processes with a high potential to be produced in a small volume. This process was patented by Leszak in 1967 and its feasibility was confirmed by Kitazawa et al., in manufacturing of rotational symmetric parts [1], [2]. In this process, simple forming tool with hemispherical-head travels on a sheet metal in a predefined path and apply local and controllable plastic deformation to create the final geometry [3-6]. On the other hand, the geometrical and dimensional accuracy of the SPIF products is incomplete. In fact, the sheet metal is clamped simply and can be bended freely during the process. Thus, when the tool pressure is removed from the sheet, three different types of error will be detected on the final geometry (Fig. 1).
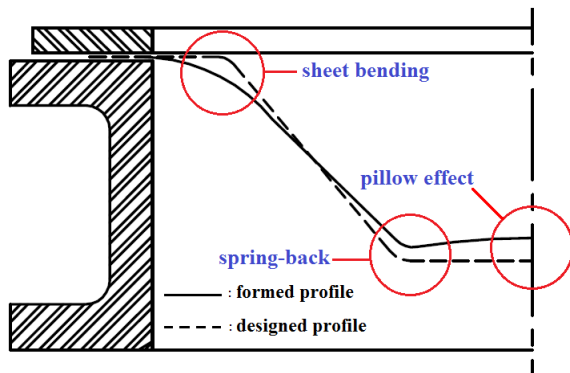

Fig. 1   Different types of error on the final geometry in SPIF process

(**1**) Sheet bending: This error occurs near the major base of the part and usually can be removed by employing backing plate, which lead to the increase of sheet rigidity.

(**2**) Lift up: In this state, the formed sheet leaps upward and the final depth of the part is less than the applied depth. This geometrical error is recognized as spring-back.

(**3**) Pillow effect: This error occurs in the minor base of the part and appears in the form of the concaved curve, which result from the undeformed material.

Micari et al., presented some strategies for reduction of geometrical and dimensional errors involved in the SPIF process [7]. They discussed on the new trends in

this direction and showed that between different suggested approaches, the ones based on the use of optimized tool trajectories seem to be the most promising. Ambrogio et al., focused on the evaluation and compensation of elastic spring-back [8]. In this way, an integrated numerical/experimental procedure was proposed in order to minimize the shape defects between the obtained geometry and the desired one. They have shown that the dimensional accuracy of the formed sample depends on the tool diameter and vertical step size. In addition, design of optimized trajectories was introduced as one of the most promising way in order to assess the profiles that are more precise.

Allwood et al., have reported that the sheet metal forming processes meet typically the geometrical tolerances in $\pm 0.2\,mm$ limit, whereas the tolerance performance of incremental forming processes, are ten times worse than this situation [9]. The weakness of geometrical accuracy in incremental forming process in comparison with CNC machining process is due to the fact that the sheet metal deformation is not defined solely by the tool path. Hence, a significant deformation is created at the outer limits of the contact zone. Ambrogio et al., performed several tests based on DOE techniques to fully understand the spring-back phenomenon with respect to other geometrical parameters such as wall inclination angle, final depth of the product and sheet thickness [10]. Subsequently, they extracted an analytical model to estimate the "over-deformation" to be applied in order to reduce the geometrical error.

Meier et al., have shown that the use of Robot in incremental forming process (Roboforming) has a high capability to enhance the geometrical accuracy [11]. They suggested two approaches (a model-based and a sensor-based approach) to determine the geometrical deviations. For both approaches, one universal compensation strategy can be used to reduce the determined deviations in Roboforming. Allwood et al., proposed the employment of partially cut-out blanks in incremental forming [12]. The use of this type of blank creates a localized deformation earlier, and as a result reduces the difference between a part made by a "contour tool path" and the target product geometry. The influence of these partial cut-outs was evaluated by forming a simple and a complex part, with and without cut-outs and with and without backing plates.

The results indicated that partially cut-out blanks lead to slightly more accurate forming than conventional blanks when unsupported, but that the accuracy improvement is less than that which is achieved by use of a stiff cut-out supporting plate. Therefore, it seems that the use of partially cut-out blanks does not give a useful benefit in incremental forming. Review of the previous researches shows that different approaches

have been made by scientists to increase the geometrical and dimensional accuracy of the formed sample. Tool path optimization, process parameters optimization and development of new methods are some of these strategies. On the other hand, the application of ultrasonic vibration in metal forming has been discussed for many years [13-15]. The experiments on superimposing the ultrasonic oscillations on the forming process indicated some benefits such as reduction of the forming forces, reduction of the flow stress, reduction of the friction between die and workpiece and production of the better surface qualities and higher precision.

Vahdati et al. [16], [17] showed that the ultrasonic excitation of hemispherical-head tool in SPIF process (UVaSPIF), reduces the average of vertical component of forming force and spring-back rate of the formed sample. Thus, the sheet metal will be formed incrementally in the presence of ultrasonic vibration with given frequency and specified amplitude as compared to the previous researches. Hence, in the present article, the analysis and optimization of spring-back phenomenon in UVaSPIF process is done based on DOE principles using RSM technique. The objectives of this research unfold on extraction of regression model and mathematical equation resulting from ANOVA for spring-back coefficient and access to optimal conditions of the experiment.

2   METHODOLOGY OF STATISTICAL ANALYSIS

A model presented in Fig. 2 can introduce the process under study. With the assumption of independency of controllable factors (X_i) and response of the process (Y_i), the goal is to obtain the mathematical relation between the output variable and the input variables with a minimum error.
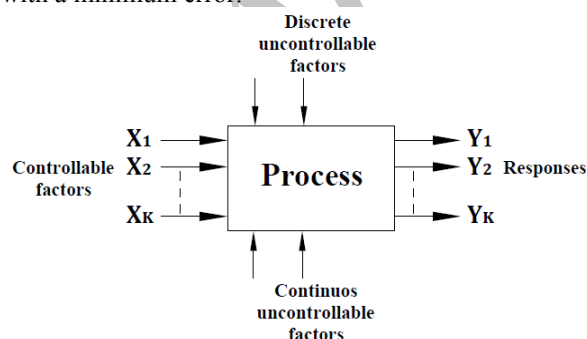

Fig. 2   General model of the process

For this purpose, the methodology of statistical analysis in this research includes the following seven steps:
(**1**): Selecting the response variable
(**2**): Selecting the controllable factors
(**3**): Selecting the experiment design
(**4**): Experiment execution
(**5**): Measuring the response variable
(**6**): Data analysis
(**7**): Optimization and confirmation

2.1. Selecting the response variable

For evaluation of the spring-back rate, a criterion namely spring-back coefficient (K) is used which can be calculated from the following relation [18]:

$$K = \frac{h_1 + \frac{t_0}{2}}{h_{ave.} + \frac{t_0}{2}} \tag{1}$$

In this relation, h_1 is the applied depth on the sample geometry; t_0 is the initial thickness of the sheet, and $h_{ave.}$ is the average of the measured depth after unclamping the formed sample. With regard to the above relation, to the extent that the K parameter becomes closer to the number one ($K \rightarrow 1$), to the same extent, it denotes the reduction of spring-back rate. Hence, in this research, the spring-back coefficient is considered as the response variable.

2.2. Selecting the controllable factors

The ultrasonic generator and transducer are the components of production and transmission of vibration in this process, respectively [16], [17]. With regard to the fact that during the process execution, the applied force on the forming tool will cause a change in the vibration conditions of the tool, so that the vibration parameters of the process such as generator power, frequency, and amplitude of vibration are considered as the uncontrollable input factors. Thus, five controllable factors of vertical step size (v), sheet thickness (t), tool diameter (d), wall inclination angle (φ) and feed rate (f) were selected as the input variables of the experiment and each of them were studied at three levels of low (-1), central (0) and high (+1). The high and low levels of each parameter are coded by +1 and -1. In addition, the coded value of each desirable middle level is calculated through the following relation [19]:

$$X = \frac{2x - (x_{max} + x_{min})}{(x_{max} - x_{min})} \tag{2}$$

In this relation, X is the coded value of concerned parameter with the actual value of x (between x_{min} and x_{max}). x_{min} and x_{max} have the actual low and high values of the parameter accordingly. Table 1 shows the input variables and experimental design levels used with coded and actual values. The variation range of these factors was determined based on the primary

experiments, which lead to safe production of the final geometry.

Table 1 Input variables with design levels

Variable	Notation	Unit	-1	0	+1
Vertical step size	v	mm	0.25	0.5	0.75
Sheet thickness	t	mm	0.4	0.7	1
Tool diameter	d	mm	10	15	20
Wall inclination angle	φ	°	40	50	60
Feed rate	f	mm/min	1500	2000	2500

2.3. Selecting the experiment design

In the present research, RSM is used as the experiment design technique. In this method, there is a set of mathematical and statistical techniques, which are useful for modeling, and analysis of the problems [20], [21]. In such problems, the relation between response and input variables is unknown. Thus, the first step in this method is to find a suitable approximation of the real relation existing between the response variable (y) and the set of input variables (x). The approximating functions are in the form of the linear and quadratic models and are written in the form of the following relations:

$$y = \beta_0 + \beta_1 x_1 + \beta_2 x_2 + ... + \beta_k x_k + \varepsilon \qquad (3)$$

$$y = \beta_0 + \sum_{i=1}^{k} \beta_i x_i + \sum_{i=1}^{k} \beta_{ii} x_i^2 + \sum_i \sum_j \beta_{ij} x_i x_j + \varepsilon \qquad (4)$$

In the above functions, β_0 is the constant value, β_i is the first-order (linear) coefficient, β_{ii} is the second-order (quadratic) coefficient, β_{ij} is the interaction coefficient, k is the number of independent variables, and ε is the rate of error. In this research, the second-order model and Box-Behnken Design (BBD) are used. The software used for experiment design and statistical analysis is Minitab [22]. Table 2 shows the design matrix with 46 tests in the form of coded runs. Five tests are repeated at the central levels of parameters (zero level).

Table 2 Design matrix with measured and calculated results

Test no.	v	t	d	φ	f	$h_{ave.}(mm)$	K
1	0	0	-1	+1	0	29.629	1.01238
2	0	0	+1	-1	0	29.602	1.01329
3	0	0	-1	0	+1	29.635	1.01217
4	0	+1	-1	0	0	29.869	1.00431
5	0	0	0	0	0	29.612	1.01295
6	0	0	0	0	0	29.612	1.01295
7	-1	0	-1	0	0	29.871	1.00427
8	0	0	0	+1	-1	29.609	1.01305
9	0	+1	0	-1	0	29.824	1.0058
10	-1	0	0	0	-1	29.827	1.00573
11	0	0	0	0	0	29.612	1.01295
12	0	+1	0	0	-1	29.821	1.0059
13	-1	-1	0	0	0	29.767	1.00778
14	0	-1	0	-1	0	29.584	1.01397
15	0	0	-1	-1	0	29.818	1.00603
16	+1	0	0	0	-1	29.557	1.01481
17	0	0	0	-1	-1	29.615	1.01285
18	0	0	0	+1	+1	29.606	1.01315
19	0	0	-1	0	-1	29.815	1.00613
20	0	-1	0	+1	0	29.566	1.01458
21	0	-1	-1	0	0	29.623	1.01264
22	+1	0	+1	0	0	29.55	1.01505
23	0	0	+1	+1	0	29.59	1.01369
24	0	0	0	0	0	29.612	1.01295
25	0	-1	+1	0	0	29.563	1.01468
26	0	+1	0	0	+1	29.687	1.01037
27	+1	0	0	0	+1	29.555	1.01488
28	+1	0	-1	0	0	29.617	1.01278
29	+1	0	0	+1	0	29.553	1.01495
30	-1	0	0	-1	0	29.83	1.00563
31	0	0	0	0	0	29.612	1.01295
32	0	+1	0	+1	0	29.682	1.01054
33	+1	0	0	-1	0	29.559	1.01474
34	0	0	0	-1	+1	29.614	1.01288
35	+1	+1	0	0	0	29.672	1.01087
36	-1	+1	0	0	0	29.873	1.00418
37	0	+1	+1	0	0	29.677	1.0107
38	0	-1	0	0	+1	29.572	1.01438
39	0	0	+1	0	+1	29.594	1.01356
40	-1	0	+1	0	0	29.771	1.0076
41	+1	-1	0	0	0	29.545	1.0153
42	-1	0	0	+1	0	29.775	1.00747
43	0	-1	0	0	-1	29.578	1.01417
44	0	0	+1	0	-1	29.598	1.01342
45	-1	0	0	0	+1	29.779	1.00734
46	0	0	0	0	0	29.612	1.01295

2.4. Experiment execution
The sheet metal is Al 1050-O, which is used in annealed form (350°c for 2 hours). The hydraulic oil (HLP68) was used as lubricator [23]. The hemispherical-head tools were designed and manufactured in three diameters of 10, 15, and 20mm (Fig. 3) in accordance with the instruction of design, manufacturing, and test of vibrating forming tools [16]. For imposing the ultrasonic vibration on the forming tools, an ultrasonic generator with power of 1000 watt and operational frequency of 20 kHz were used. The amplitude of vibration of forming tools was measured to be 7.5 microns. The circular speed of forming tools was adjusted in 125rpm. Figure 4 shows the fixture components in SPIF process. The sheet metal is placed between clamping plate and backing plate. The sample geometry was considered in the form of pyramid frustum with the base dimension of 80×80mm and depth of 30mm (Fig. 5).
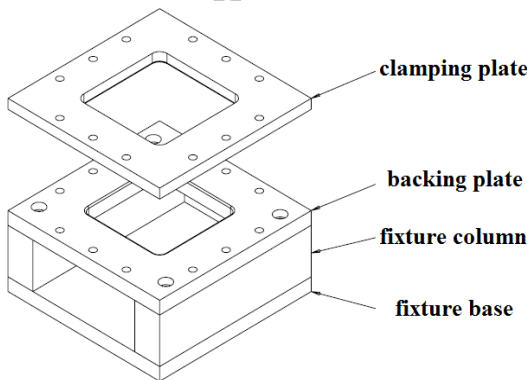

Fig. 3   Forming tools

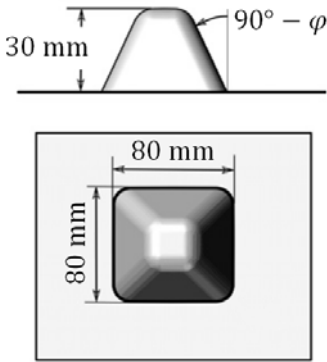**Fig. 4**   Components of the fixture in SPIF process

Fig. 5   Dimensional characteristics of the formed sample

Tool path strategy is in the form of the gradual imposing of wall inclination angle (based on successive horizontal-vertical steps in one face of sample geometry) and then the linear motion in the working plane (Fig. 6). Figure 7 shows the simulation of tool path strategy in Cimco software for the wall inclination angle of $\varphi = 60°$ [24]. The tests were performed in accordance with the 46 runs included in the Table 2. The samples were formed in accordance with the concerned geometry and strategy. Figure 8 shows the two formed samples in experimental tests.
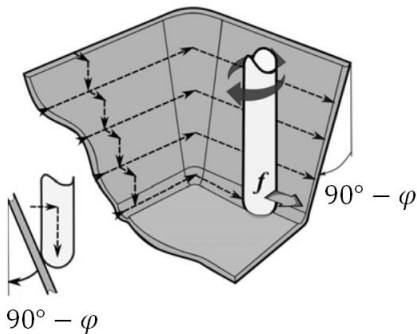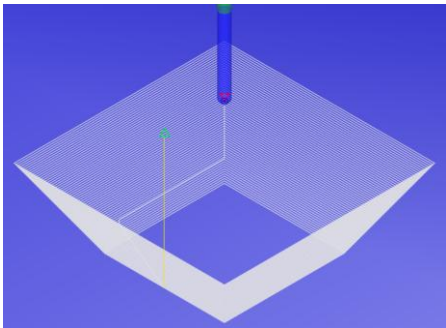

Fig. 6   Tool path strategy

Fig. 7   Simulation of tool path strategy

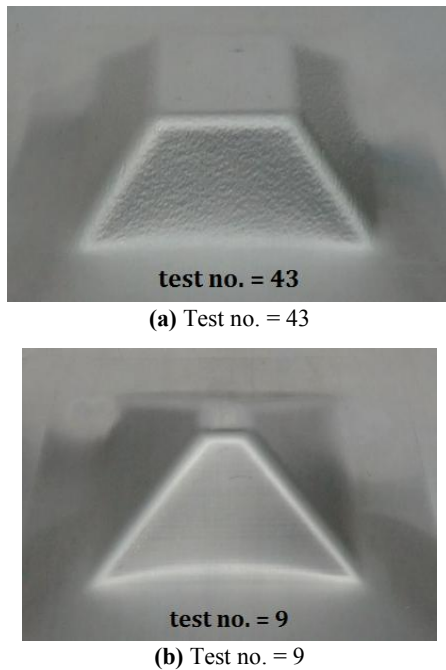**(a)** Test no. = 43

(b) Test no. = 9

Fig. 8   Two formed samples in the experimental tests

2.5. Measuring the response variable

The depth of formed samples was measured in the position of spring-back creation by the Contourgraph system and its average was registered as the $h_{ave.}$ (Fig. 9). Table 2 shows the results of measuring ($h_{ave.}$) and calculation of the spring-back coefficient (K) of the formed samples.
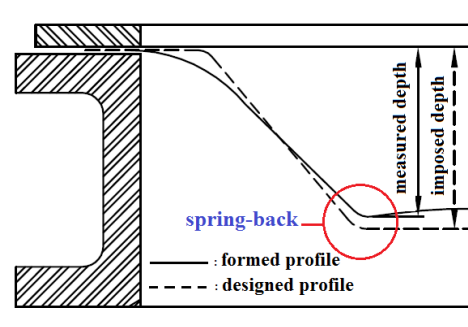
2.6. Data analysis

Analysis of experimental data is performed by ANOVA, which is a powerful tool to study the importance of a parameter and identify the significance of its effect. In addition, in order to create the mathematical functions between the response variable and the effective parameters, the regression analysis is employed [19]. Confidence level (α) is considered as equal to 0.05 and statistically, it means that the final model can predict the data with an error less than 5%.

The effectiveness of a term is specified through " $P-value$ ", related to the corresponding term. Thus, the terms are identified with the " $P-value \leq \alpha$ ", as significant and with the " $P-value > \alpha$ ", as insignificant. To the extent that the " $P-value$ " related to a term is smaller, to the same extent the significance of that term in the model is greater. Thus, with the assumption of $\alpha = 0.05$ and based on the primary obtained results from ANOVA, the first-order parameters: vertical step size (v), sheet thickness (t), tool diameter (d), wall inclination angle (φ) and feed rate (f), the second-order terms: v^2 , t^2 , d^2 and

interactional terms: td , $t\varphi$, tf , $d\varphi$ and df were determined as the effective terms on the spring-back coefficient and the other terms as the ineffective terms.
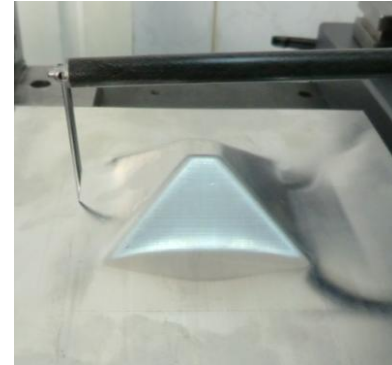
(a) Plunger motion on the sample surface

(b) Difference between the imposed and measured depth

Fig. 9   Measuring the depth of formed sample

In the final step of data analysis, the terms with inactive effects should be removed from the model and just the terms with active effects to be analyzed. Thus, all ineffective terms with the " $P-value > 0.05$ " are deleted from the analysis and all terms with the " $P-value \leq 0.05$ " in the final step of ANOVA will be present. Table 3 shows the regression table, which is the result from the final ANOVA, based on the effective terms.

As it is observed, all terms existing in Table 3 have appeared with the " $P-value \leq 0.05$ ", and as effective terms on the response variable. The emergence of positive sign (+) for regression coefficients, states the presence of a direct relation between the terms and response variable. Whereas, the emergence of negative sign (-) for regression coefficients shows the presence of a reverse relation between the terms and response variable. In the continuation, the role of the effective parameters for achieving an ideal situation of the response variable will be studied. Thus, the reduction of spring-back coefficient (K) is determined as the ideal situation.

Table 3   Regression table based on the effective terms

Term	Regression coefficient	T-value	P-value
Constant	1.01273	4588.851	0
v	0.00396	19.188	0
t	-0.0028	-13.572	0
d	0.00195	9.47	0
φ	0.00091	4.426	0
f	0.00079	3.836	0.001
$v \times v$	-0.0019	-7.244	0
$t \times t$	-0.00134	-5.09	0
$d \times d$	-0.00113	-4.288	0
$t \times d$	0.00109	2.634	0.013
$t \times \varphi$	0.00103	2.501	0.018
$t \times f$	0.00106	2.579	0.015
$d \times \varphi$	-0.00149	-3.603	0.001
$d \times f$	-0.00148	-3.572	0.001

$R^2 = 96.13\%$ $R^2_{adjusted} = 94.56\%$

The following relation expresses the regression equation of spring-back coefficient as a function of the coded effective values:

$$K = 1.01273 + 0.00396v - 0.0028t + 0.00195d$$
$$+ 0.00091\varphi + 0.00079f - 0.0019v^2$$
$$- 0.00134t^2 - 0.00113d^2 + 0.00109td \qquad (5)$$
$$+ 0.00103t\varphi + 0.00106tf - 0.00149d\varphi$$
$$- 0.00148df$$

The investigation of the T-value belonging to the effective terms shows that:

(**1**): Vertical step size (v) as the linear effect has the greatest effect and the product of sheet thickness and wall inclination angle ($t\varphi$) as the interactional effect, has the least effect on the spring-back coefficient. In other words, the effect of v is 7.6 times of the $t\varphi$ effect.

(**2**): Vertical step size (v) among the linear effects has the greatest effect on the spring-back coefficient.

(**3**): Vertical step size (v) among the quadratic effects (v^2) has the greatest effect on the spring-back coefficient.

(**4**): The product of tool diameter and wall inclination angle ($d\varphi$) and the product of tool diameter and feed rate (df) among the interactional effects have the greatest effect on the spring-back coefficient.

As it is observed in Table 3, the correlation coefficients of R^2 and R^2_{adj} show the peak values of 96% and 94% respectively. As a result, a high correlation is established between the observed data in the experimental tests and the predicted responses resulting from the regression equation. Hence, the ability of the fitted model and accuracy of the regression equation in describing and predicting the changes of the response variable are confirmed. Table 4 shows the obtained results from the ANOVA.

Table 4   ANOVA results for the final model

Source of variation	Degree of freedom	F-value	P-value
Regression	13	61.21	0
Linear	5	135.28	0
v	1	368.19	0
t	1	184.21	0
d	1	89.68	0
φ	1	19.59	0
f	1	14.71	0.001
Square	3	24.58	0
$v \times v$	1	52.48	0
$t \times t$	1	25.91	0
$d \times d$	1	18.38	0
Interaction	5	9.12	0
$t \times d$	1	6.94	0.013
$t \times \varphi$	1	6.25	0.018
$t \times f$	1	6.65	0.015
$d \times \varphi$	1	12.98	0.001
$d \times f$	1	12.76	0.001
Residual Error	32	-	-
Lack of Fit	27	1.432	0.093
Pure Error	5	-	-
Total	45	-	-

In order to investigate the accuracy of the regression model, in addition to R^2 evaluation, the Lack of Fit (LOF) test is also used. The significance of this test ($P - value_{LOF} \leq 0.05$) indicates that the data are not well placed around the model and it is not possible to use the model to predict the response variable. Thus, with the confirmation of the insignificance of the LOF test ($P - value_{LOF} > 0.05$), it is possible to find out that the model can be well fitted on the data. As it is observed in the Table 4, LOF test for the response variable is not significant and consequently, the presented model shows the data trends well. On the

other hand, the best analysis is performed when the regression is effective and the LOF is ineffective concurrently [19]. Thus, with regard to the $P-value$, it is observed that the regression term, is effective and the LOF term is ineffective.

The plot of normal probability is a useful means to check the accuracy of normal distribution of the residuals. The residual is defined in the form of the difference between the measured response in the experimental test and the predicted response by the final model. The obtained results from this research show that the residuals in this plot generally follow a straight line and there is no evidence on abnormality, asymmetry, and divergence (Fig. 10). Also, it is possible to investigate the model competency by studying the behavior of the residuals. If the regression model is appropriate, subsequently the residuals have no structure. As it is shown in Fig. 11, the residuals have been distributed randomly around the zero axis and the diagram does not include any specific pattern, hence the final model is reliable and suitable.
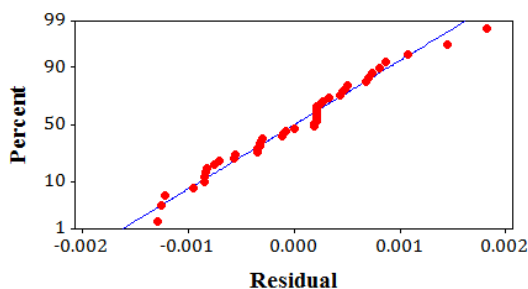

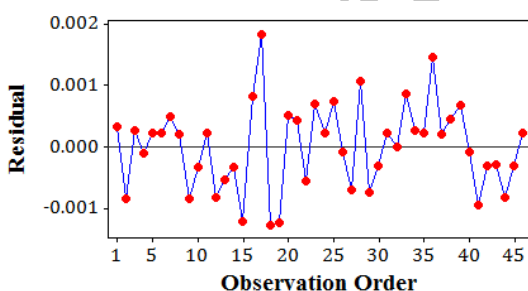**Fig. 10**   Normal probability plot

Fig. 11   Residual plot

The response behavior can be shown in terms of input variables in the form of 3D diagrams (surface plot) and 2D diagrams (contour plot). In these diagrams, the interactional effects of the two input variables on the response variable are observable and the values of other input variables are considered fixed at the central levels (zero level). The relationship of the spring-back coefficient with vertical step size (v) and tool diameter

(d) has been shown in Fig. 12. As it is observed, the reduction of tool diameter (d) causes the reduction of spring-back coefficient and this effect is intensified with the reduction of vertical step size (v).
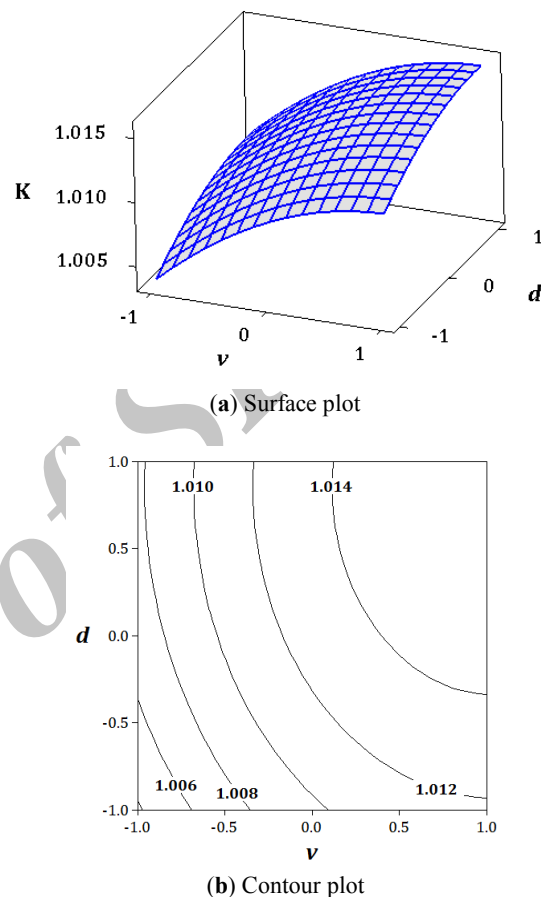

(**a**) Surface plot

(**b**) Contour plot

Fig. 12   Relationship of the spring-back coefficient (K) with vertical step size (v) and tool diameter (d)

On the other hand, the increase of sheet thickness (t) along with the reduction of wall inclination angle (φ), causes the reduction of spring-back coefficient (Fig. 13).

2.7. Optimization and confirmation
In this research, desirability method was used as the optimization technique with regard to the simplicity, flexibility, and accessibility in the software. Drringer and Suich introduced this method in 1980 [25]. In this technique, first the output response of y_i is converted into dimensionless desirability of d_i ($0 < d_i < 1$), such that the higher value of d_i signifies the greater desirability of y_i and if the response is outside the acceptable limit, $d_i = 0$.
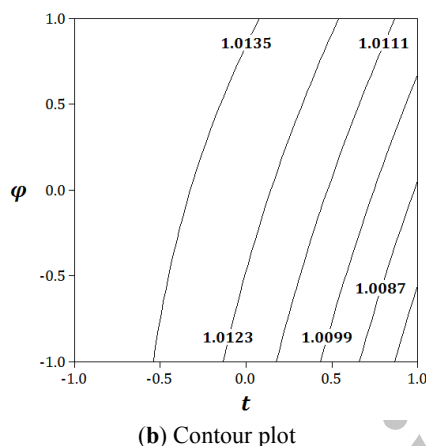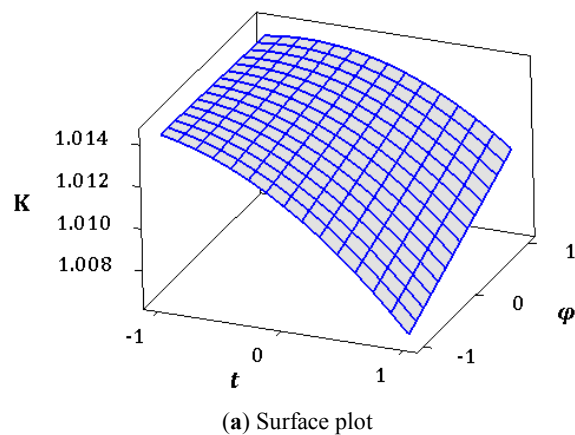
(**a**) Surface plot

(**b**) Contour plot

Fig. 13   Relationship of the spring-back coefficient (K)
with sheet thickness (t) and wall inclination angle (φ)

Thus, for the output response, a separate desirability function with a range of 0 to 1 is obtained. In this research, the goal of the desirability function is the minimization of the response variable (reduction of spring-back coefficient), where the desirability is defined in the following form:

$$d = \begin{cases} 1 & y < L \\ \left(\dfrac{U - y}{U - L}\right)^r & L \leq y \leq U \\ 0 & y > U \end{cases} \qquad (6)$$

In the above relation, L and U are the low and high limits of y, respectively. The shape of desirability function depends on the weight field (r) which is used to express the degree of significance of the target value. Here, the weight value is assumed equal to one ($r = 1$) and consequently, the desirability function is defined in a linear mode. Table 5 shows the specifications of the desirability function for the output response.

Table 5   Specifications of the desirability function

Output response	Desirability function	Function target	Weight value (r)
$y = K$	$d(y)$	$K = 1$	1

Figure 14 shows the diagrams of the spring-back coefficient model which is the resultant of the optimization process at the optimal point. As it is observed, the vertical line in red color shows the optimal values of input variables and the horizontal line in blue color shows the optimal value of output response. Thus, the effect of the input variables to achieve the target of function is identifiable and interpretable from diagram simply.
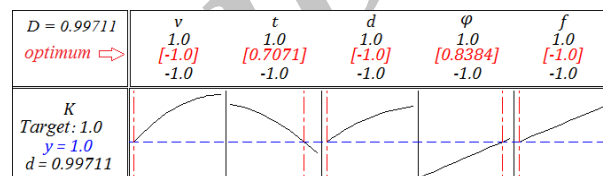

Fig. 14   Behavior of the spring-back coefficient (K) at the optimal points of input parameters

Table 6   Optimal values of the input variables

Input variable	Coded optimal value	Actual optimal value
v	-1	0.25 mm
t	0.7071	0.91 mm
d	-1	10 mm
φ	0.8384	58.38^0
f	-1	1500 mm/min

Table 6 shows the optimal values of the input variables to achieve the desirability function target. Therefore, the reduction of vertical step size (v), tool diameter (d) and feed rate (f) along with the increase of sheet thickness (t) and wall inclination angle (φ) leads to the reduction of spring-back coefficient. As it is observed, the optimal angle of wall inclination (φ) was determined to be 58.38°. Also, the optimal value of output response, which results from the regression equation is equal to one (1) and the value of the corresponding desirability function with it, is equal to 0.9971. Hence, with regard to the high value of separate desirability function, it can be realized that the procedure of process optimization has well fulfilled a pre-determined target successfully.

In order to confirm the optimized response and to measure the accuracy of the presented model, the experimental test was conducted by the finest

conditions of input variables. Table 7 shows the input variables of the test and Fig. 15 shows the formed sample after performing the confirmation test. Table 8 presents the obtained results from the confirmation test and its comparison with the optimized result.

Table 7   Input variables of the confirmation test

variable	value
v	0.25 mm
t	0.9 mm
d	10 mm
φ	58^0
f	1500 mm/min

(**a**) 3D view

(**b**) Front view

Fig. 15   Formed sample in the confirmation test

Table 8   Comparison between the obtained results from confirmation test and optimization process

K (confirmation test)	K (optimization process)	Difference percent
1.00512	1	0.51 %

This comparison shows that the error of regression model to predict the spring-back coefficient is less than 1%. Thus, the accuracy of regression model to predict the response variable is confirmed.

3   CONCLUSION

In this article, analysis and optimization of the spring-back phenomenon in the UVaSPIF process was conducted based on DOE principles using RSM technique. The major accomplishments of this research are summarized as follows:

- The primary achieved results from ANOVA with the assumption of $\alpha = 0.05$ showed that the linear terms: vertical step size (v), sheet thickness (t), tool diameter (d), wall inclination angle (φ) and feed rate (f), the quadratic terms: v^2, t^2, d^2 and the interactional terms: td, $t\varphi$, tf, $d\varphi$ and df, can have effect on the spring-back phenomenon.

- The regression equation, which results from ANOVA, was extracted to predict the spring-back coefficient in UVaSPIF process. The competency of the final model was investigated by the correlation coefficients, Lack of Fit (LOF) test, normal probability plot, and diagram of residuals. Consequently, the ability of the fitted model and accuracy of the regression equation in describing and predicting the behavior of spring-back coefficient was confirmed.

- In this research, with regard to the comprehensiveness of the presented mathematical model, a broad range of effective factors on the spring-back phenomenon is covered. Thus, the presented model can be utilized in SPIF and TPIF processes in addition to prediction and control of spring-back parameters in UVaSPIF process.

- The optimal values of input variables were extracted to access the least spring-back coefficient. The optimization results indicated that the reduction of vertical step size, tool diameter, and feed rate along with the enhancement of sheet thickness and wall inclination angle, lead to the reduction of spring-back coefficient. Also, the optimal angle of wall inclination was determined to be 58.38°.

- The high value of the desirability function corresponding to the spring-back coefficient ($d = 0.9971$), exhibited that the optimization procedure of the process has successfully fulfilled a pre-determined target.

- A comparison between the achieved results from the confirmation test and the optimization process showed that the error of regression model for prediction of spring-back coefficient is less than 1%. This proves the accuracy of proposed regression model.

REFERENCES

[1] Leszak, E., U.S. Patent Application for a "Apparatus and process for incremental dieless forming", Docket No. 3342051A, filed 1967.

[2] Kitazawa, K., Wakabayashi, A., Murata, K., and Yaejima, K., "Metal-flow phenomena in computerized numerically controlled incremental stretch-expanding of aluminium sheets", Journal of Japan Institute of Light Metals, Vol. 46, 1996, pp. 65-70.

[3] Petek, A., Jurisevic, B., Kuzman, K., and Junkar, M., "Comparison of alternative approaches of single point incremental forming processes", Journal of Materials Processing Technology, Vol. 209, 2009, pp. 1810-1815.

[4] Duflou, J., Tunckol, Y., Szekeres, A., and Vanherck, P., "Experimental study on force measurements for single point incremental forming", Journal of Materials Processing Technology, Vol. 189, 2007, pp. 65-72.

[5] Jeswiet, J., Micari, F., Hirt, G., Bramley, A., Duflou, J., and Allwood, J., "Asymmetric single point incremental forming of sheet metal", CIRP Annals - Manufacturing Technology, Vol. 54, No. 2, 2005, pp. 623-649.

[6] Thibaud, S., Ben Hmida, R., Richard, F., and Malécot, P., "A fully parametric toolbox for the simulation of single point incremental sheet forming process: Numerical feasibility and experimental validation", Simulation Modelling Practice and Theory, Vol. 29, 2012, pp. 32-43.

[7] Micari, F., Ambrogio, G., and Filice, L., "Shape and dimensional accuracy in Single Point Incremental Forming: State of the art and future trends", Journal of Materials Processing Technology, Vol. 191, 2007, pp. 390-395.

[8] Ambrogio, G., Costantino, I., De Napoli, L., Filice, L., and Muzzupappa, M., "Influence of some relevant process parameters on the dimensional accuracy in incremental forming: a numerical and experimental investigation", Journal of Materials Processing Technology, Vol. 153C/154C, 2004, pp. 501-507.

[9] Allwood, J. M., King, G. P. F., and Duflou, J., "A structured search for applications of the incremental sheet-forming process by product segmentation", Proceedings of the Institution of Mechanical Engineers, Part B: Journal of Engineering Manufacture, Vol. 219, No. 2, 2005, pp. 239-244.

[10] Ambrogio, G., Cozza, V., Filice, L., and Micari, F., "An analytical model for improving precision in single point incremental forming", Journal of Materials Processing Technology, Vol. 191, 2007, pp. 92-95.

[11] Meier, H., Buff, B., Laurischkat, R., and Smukala, V., "Increasing the part accuracy in dieless robot-based incremental sheet metal forming", CIRP Annals - Manufacturing Technology, Vol. 58, 2009, pp. 233-238.

[12] Allwood, J. M., Braun, D., and Music, O., "The effect of partially cut-out blanks on geometric accuracy in incremental sheet Forming", Journal of Materials Processing Technology, Vol. 210, 2010, pp. 1501-1510.

[13] Siegert, K., Ulmer, J., "Superimposing ultrasonic waves on the dies in tube and wire drawing", Journal of Engineering Materials and Technology, Vol. 123, 2001, pp. 517-523.

[14] Hung, J.-C., Hung, C., "The influence of ultrasonic-vibration on hot upsetting of aluminum alloy", Ultrasonics, No. 43, 2005, pp. 692-698.

[15] Tolga Bozdana, A., Gindy, N. N. Z., and Li, H., "Deep cold rolling with ultrasonic vibrations – a new mechanical surface enhancement technique", International Journal of Machine Tools and Manufacture, No. 45, 2005, pp. 713-718.

[16] Vahdati, M., Mahdavinejad, R. A., Amini, S., Abdullah, A., and Abrinia, K., "Design and manufacture of vibratory forming tool to develop "ultrasonic vibration assisted incremental sheet metal forming" process", Modares Mechanical Engineering, Vol. 14, No. 11, 2014, pp. 68-76 (In Persian).

[17] Vahdati, M., Mahdavinejad, R. A., and Amini, S., "Investigation of the Ultrasonic Vibration Effect in Incremental Sheet Metal Forming (ISMF) Process", Proceedings of the Institution of Mechanical Engineers, Part B: Journal of Engineering Manufacture, (to be published).

[18] Vahdati, M., Sedighi, M., and Khoshkish, H., "An analytical model to reduce spring back in Incremental Sheet Metal Forming (ISMF) process", International Journal of Advanced Materials Research (AMR), Vols. 83-86, 2010, pp. 1113-1120.

[19] Montgomery, D. C., "Design and Analysis of Experiments", 3rd ed., New York, John Wiley & Sons, 1991.

[20] Khuri, A. I., Cornell, J. A., "Response Surfaces Design and Analysis", 2nd ed., New York, Marcel Dekker, 1996.

[21] Myers, R. H., Montgomery, D. C., "Response Surface Methodology: Process and Product Optimization Using Designed Experiments", 2nd ed., New York, John Wiley & Sons, 2002.

[22] Minitab Software Package, Ver. 16, http://www.minitab.com.

[23] DIN 51524, Part 2.

[24] CIMCO Software Package, Ver. 5, http://www.cimco.com.

[25] Myers, R. H., Montgomery, D. C., and Anderson-Cook, C. M., "Response Surface Methodology: Process and Product Optimization Using Designed Experiments", 3rd ed., New York, John Wiley & Sons, 2009.